Amorphous silica-alumina – perspective supports for selective hydrotreating of FCC gasoline: Influence of Mg

K.A. Nadeina*, O.V. Klimov, I.G. Danilova, V.Yu. Pereyma, E.Yu. Gerasimov, I.P. Prosvirin, A.S. Noskov

Boreskov Institute of Catalysis, Siberian Branch, Russian Academy of Sciences, 630090, Novosibirsk, pr. ak. Lavrentiev 5, Russia

ARTICLE INFO

ABSTRACT

CoMo/Al$_2$O$_3$-ASA catalysts with Mg were synthesized. Catalysts differed in the way of Mg addition: 1. Mg was added to ASA, 2. Mg was added to the kneading paste during the support preparation, 3. Mg was added before or after Co and Mo by the impregnation. Catalysts were characterized by the following techniques: low-temperature N$_2$ adsorption, IR of CO and CO$_2$ adsorption, X-ray photoelectron spectroscopy, high-resolution transmission electron microscopy. Synthesized catalysts were tested in hydrotreating of the model fluid catalytic cracking gasoline containing 250 ppm of sulfur from thiophene, 40 wt.% of toluene, 40 wt.% of heptane and 20 wt.% of *n*-hexene-1. It was found that the addition of Mg resulted in changes of physico-chemical properties of catalysts and their HDS and HYD activities. The way of Mg addition influenced the content of Lewis and Brønsted acid sites and morphology of sulfide active component. Mg increased HDS activity and decreased octane number loss. The catalysts with Mg in the kneading paste of the support and with Mg added after active metals showed the best combination of HDS activity and selectivity.

1. Introduction

Catalytic cracking of heavy oil distillates refers to the processes that contribute 30–50% of gasoline to gasoline pool [1]. Fluid catalytic cracking gasoline (FCC gasoline) contains 20–40 wt.% of olefins, which provide a high octane number (up to 92 points). However, FCC gasoline is generally responsible for more than 90% of the sulfur compounds in the engine gasoline. The urgent demand to reduce exhaust emissions from gasoline-powered motor vehicles makes it necessary to control the sulfur content in gasoline.

Hydrotreating is the main process to decrease sulfur content in oil distillates. Since the initial research octane number of FCC gasolines does not usually exceed 93 points, it is possible to admit the decrease in the octane number during hydrotreating by less than 1–2 points. Otherwise, hydrotreated FCC gasoline is not suitable for obtaining commercial gasoline with a research octane number of at least 95. There are different variations of hydrotreating process for selective hydrotreating of FCC gasoline. They are based on separate desulfurization of light and heavy gasoline fractions. Many of these processes are technologically complex and power-consuming. On the other hand, hydrotreating of FCC gasoline without previous fractionation results in the octane number decrease by at least 2 points. The main reason for the octane number decrease is the use of non-selective catalysts, which along with the desired desulfurization reactions of sulfur containing compounds catalyze undesirable hydrogenation reactions of high octane olefins. Therefore, there is an urgency for new catalysts characterized by increased activity in hydrogenolysis reactions of sulfur-containing compounds, with minimal activity in the hydrogenation of high-octane olefins. Therefore, the search of new solutions, such as development of new selective catalytic systems, plays an important role in the production of ultra-low sulfur gasoline.

Currently, a large amount of scientific information on the composition and structure of the sulfide active component of hydrotreating catalysts has been accumulated. In accordance with generally accepted concepts, the active component of hydrotreating catalysts comprises molybdenum sulfide particles decorated with cobalt atoms [2]. The main difference between the sulfide active component in the catalysts for the hydrotreating of FCC gasoline from hydrotreating catalysts of other fractions is its selectivity, expressed in the ratio of the rates of target hydrogenolysis reactions of sulfur-containing compounds and undesired reactions of olefin hydrogenation. The degree of the saturation of olefins during hydrotreating of FCC gasoline over selective and unselective cat-

* Corresponding author.
E-mail address: lakmallow@catalysis.ru (K.A. Nadeina).

alysts at equal desulfurisation degree can differ up to 4 times [3]. A number of studies have shown [4–6] that the selectivity of catalysts in hydrogenation reactions is almost completely determined by the properties of the sulfide active component and depends little on the nature of the support. The selectivity of the cobalt (nickel)-molybdenum (tungsten) hydrotreating catalysts without modifying agents is influenced by three parameters: a) atomic ratios of Co/Mo or Co/Mo/W in the sulfide active component [3,7]; b) concentration of active component in the catalyst [8]; c) the dispersion of the active component, which is determined by the linear dimensions of its particles and the stacking number of the CoMoS phase [5,9,10].

However, other studies have shown that the addition of modifying additives to the catalyst allows one to influence the properties of the active phase or directly affect the activity of the catalyst in certain reactions. Thus, the catalysts with amorphous silica-alumina (ASA) supports were shown to have high selectivity in hydrotreating of FCC gasoline [11,12]. High isomerization activity of high-reactive high-octane olefins into low-reactive high-octane derivatives provided high selectivity of these catalysts. However, the use of ASA in supports of hydrotreating catalysts has some disadvantages, for example, sufficiently low mechanical strength, that makes it necessary to use binding agent. Moreover, increase of ASA content in the catalyst will inevitably increase the cost. Therefore, the question arises whether it is possible to increase the selectivity of the catalysts based on amorphous silica-alumina?

In order to increase the selectivity of catalysts for the hydrotreating of FCC gasolines, in particular to suppress undesirable reactions of hydrogenation of high-octane olefins, catalysts are modified by various acidic or alkaline components. Alkali metal compounds – sodium, potassium and magnesium, are most often used. A number of studies have not revealed a clear effect of modifying alkaline additives on the state of metals in the composition of the active component [4,5,10], but only an indirect effect on the morphology of the CoMoS particles is shown, which is more dependent on other factors. It was shown in [13] that the addition of Na additive to the catalyst composition resulted in a strong decrease in both the hydrogenating and desulfurisation activitied that was not favorable for the FCC hydrotreating catalysts. On the contrary, it was shown in [14], that when potassium was introduced into CoMo catalysts based on Al_2O_3 or hydrotalcite, there was a slight decrease in desulfurizing activity and a sharp decrease in hydrogenating activity and a proportional increase in a selectivity factor. The introduction of 2.7 wt.% K into the industrial $CoMo/Al_2O_3$ catalyst HR306 results in a sharp increase in the selectivity of the hydrotreating, but the desulphurization activity was somewhat reduced [15]. Thus, the data published in the literature suggest that the modification of $CoMo/Al_2O_3$ by alkaline additives slightly increases the selectivity of the catalysts for the hydrotreating of FCC gasoline. However, they almost always reduces the desulfurization activity. The main reason is that addition of alkali metals have slight positive effect on electronic properties of the active component or, on the contrary, blocks sites of desulfurization [16,17]. The effect on the support consists in changing the acid properties of the already formed surface, and practically does not affect the structure of the support itself. Consequently, when modifying the support or the catalyst with alkali metal compounds, one should not expect a sharp positive effect, ultimately resulting in the preservation of the octane number of FCC gasolines during their hydrotreating. A much greater positive effect should be given either to the use of components that radically alter the structure of the support, or to use additives that already have a structure. Mg compounds, whose introduction into the support can results in the formation of surface spinel-like structures, are promising as such additives. The structure and acid properties of Mg spinel-like structures differ fundamentally from the properties

of alumina, and, at the same time, they remain in the composition of granular supports and catalysts.

The use of Mg hydrotalcites as components of a composite support (Al_2O_3/hydrotalcite weight ratio = 1/3) in Co-Mo FCC hydrotreating catalysts is described in [14]. The authors found that although hydrotalcite-based catalysts are somewhat inferior in hydrodesulfurization activity to the catalyst based on Al_2O_3, they are characterized by high selectivity and, as a consequence, greater preservation of the octane number. This allows us to consider hydrotalcites as promising components in the preparation of supports for selective hydrotreating catalysts. However, the preparation of supports generally includes a calcination step at a temperature of about 550°C. At this temperature, hydrotalcite decomposes to form mixed aluminas and, for example, magnesium. Accordingly, it is possible that the support, and further a catalyst with similar properties, can be obtained from other Mg and Al compounds, excluding the synthesis stage of the hydrotalcite itself. In addition, the introduction of Mg compounds to a support or catalyst based on alumina or amorphous aluminosilicate can results in the formation of hydrotalcites and at the same time have a positive effect on the structural and catalytic characteristics of the support and the catalyst as a whole. On top of that several patents recommended the use of MgO-supported catalysts for the selective HDS of FCC gasoline [18,19]. It is believed that Mg forms sites with their own acid-base properties that changes morphology of active component and, therefore increases proportion of hydrodesulfurization sites to hydrogenation one [20]. Among these, catalysts containing Mg in their composition, besides the conventional CoMo components, were found to be promising for preparation of hydrotreating catalysts of FCC gasoline. However, most works, which are devoted to the influence of Mg, refer to $CoMo/Al_2O_3$-MgO. Influence of Mg on catalysts with silica containing supports is not present in the literature.

In this investigation, we attempted to increase selectivity of $CoMo/ASA-Al_2O_3$ catalysts for FCC gasoline selective HDS, investigated the physicochemical properties of catalysts with Mg and the selective HDS performance thereof, and presented a reasonable explanation for the enhancement of HDS selectivity.

2. Experimental

2.1. Preparation of supports and catalysts

Initial amorphous silica-alumina powder (hereinafter ASA) with ratio Si/(Si + Al) = 0.5 was prepared as it was described in [21]. Supports were prepared by extrusion of paste containing ASA and boehmite (Sasol, Germany GmbH) powders. Boehmite was used as a binding agent to form trilobe extrudates. Ratio of aluminosilicate/boehmite was 70/30.

Catalysts were prepared by impregnation of the supports with the solution containing ammonium heptamolibdate $NH_4Mo_7O_{24} \cdot 4H_2O$ and cobalt nitrate $Co(NO_3)_2 \cdot 6H_2O$ followed by drying at 120°C and calcination at 550°C. Content of active metals in final catalyst was the following: Mo – 3.3 ± 0.3 wt. % and Co – 0.7 ± 0.1 wt. %. Co to Mo ratio is 0.2 in the catalysts.

Mg was added at different stages: 1. during preparation of ASA; 2. during preparation of the kneading paste of the support; 3. before the impregnation of the support by Co and Mo compounds (by the impregnation of the support with $Mg(NO_3)_2$ solution followed by drying and calcination); 4. after the impregnation of the support by Co and Mo compounds (by impregnation of the support with $Mg(NO_3)_2$ solution followed by drying and calcination). Mg content was about 1 wt.% in all the samples.

Also, $CoMo/ASA-Al_2O_3$ without Mg were prepared for comparison.

Finally, the following samples were prepared:

Catalyst	Ways of Mg addition
CoMo/(Al + ASA)	No Mg
CoMo/(Al + MgASA)	Mg in ASA
CoMo/(Al + ASA + Mg)	Mg in support
CoMoMg/AlASA	Mg is added after CoMo
MgCoMo/AlASA	Mg is added before CoMo

2.2. Sulfiding and testing of catalysts

Catalysts were crushed to a particle size 0.25–0.5 mm and sulfided under atmospheric pressure in H_2S flow (500 h^{-1}). Sulfiding was carried out in two steps − 2 h at 200°C and 2 h at 400°C.

All catalysts were tested in hydrotreating of model fuel. Hydrotreating of model feed was carried out in a fixed bed reactor in the following conditions: LHSV = 10.0 h^{-1}, T = 220 and 240° C, P = 2.5 MPa, $nm^3 H_2/m^3 feed$ = 200. The composition of model feed was the following: thiophene − 250 ppm in terms of S, toluene − 40%, heptane − 40%, 1-hexene − 20%. In such conditions the weight liquid product output was 94–98%. Composition of gas and liquid products was analysed by chromatograph analyzer Arnel 4050 Perkin Elmer Clarus equipped by capillary column Rtx-DHA 100м, 0.25мм ID, 0.5мкм.

3. Investigation techniques

3.1. Nitrogen adsorption-desorption

The textural properties of the catalyst and support were determined by nitrogen physisorption using an ASAP 2400 (USA) instrument. Prior to analysis, samples were subjected to a N_2 flow at 200°C for 2 h. The BET surface areas were calculated from the nitrogen uptakes at relative pressures ranging from 0.05 to 0.30. The total pore volume was derived from the amount of nitrogen adsorbed at a relative pressure close to unity (in practice, P/P_0 = 0.995) by assuming that all accessible pores had been filled with condensed nitrogen in the normal liquid state. The pore size distribution was calculated using the BJH method using the adsorption and desorption branches of the isotherm.

3.2. HRTEM

HRTEM images were obtained by a JEM-2010 electron microscope (JEOL, Japan) with a lattice-fringe resolution of 0.14 nm at an accelerating voltage of 200 kV. The high-resolution images of the periodic structures were analysed by the Fourier method. Samples for HRTEM examination were prepared on a perforated carbon film mounted on a copper grid. The particle size of the initial AlOOH powders and the slab length of the sulfide active component were defined using the average data for at least 500 particles.

3.3. XPS

X-ray photoelectron spectra (XPS) were measured using a SPECS spectrometer (Germany) with a PHOIBOS-150 hemispherical energy analyser and Mg Kα irradiation ($h\nu$ = 1253.6 eV, 200 W). The binding energy scale was preliminarily calibrated using the peak positions of the $Au4f_{7/2}$ (84.0 eV) and $Cu2p_{3/2}$ (932.67 eV) core levels. The samples were supported using conductive scotch tape. The internal reference method was used for the correct calibration of the photoelectron peaks. $Al2p$ (E_b = 74.6 eV) and $Al2s$ (E_b = 119.4 eV) lines were used for calibration. A low-energy electron gun (FG-15/40, SPECS) was used for the sample charge neutralization.

3.4. IR-spectroscopy of adsorbed CO

The acidic properties of catalysts in the oxide state and initial ASA were studied by Infra-red spectroscopy (IR) with the use of the low temperature adsorption of CO molecule [22,23].

IR spectra were recorded on a Shimadzu FTIR-8300 spectrometer within the spectral range of 700–6000 cm^{-1} with a resolution of 4 cm^{-1} and 300 scans for signal accumulation. The powder samples were pressed into thin self-supporting wafers (0.006–0.015 g/cm^2) and activated in the special IR cell at 773 K for 2 h in dynamic vacuum of 10^{-3} mbar. Spectra were registered at the room temperature, after then samples were cooled to liquid nitrogen temperature and kept at this temperature 20–30 min. CO was introduced at liquid nitrogen temperature by doses up to an equilibrium pressure of 13 mbar and following desorption was performed by heating to room temperature. The spectrum at the pressure of 13 mbar CO were recorded at 293 K too. After deconvolution of the corresponding IR bands into individual Gauss components by home-made program, the concentration of Lewis acidic sites (LASs) was evaluated from the integral intensity (A) of CO band in the range of 2180–2240 cm^{-1} using the equation: $C = A/A_0$. The following molar integral absorption coefficients values (A_0, cm/mmol) were used: 1.23 (2230–2220 cm^{-1}), 1.1 (2216–2206 cm^{-1}), 0.9 (2198–2180 cm^{-1}) [23]. A value of the upward ν_{CO} frequency shift determines the strength of Lewis acid sites, as it is related to the heat of complex formation by the following formula: Q_{CO} [kJ/mol] = 10.5 + 0.5(ν_{co-} = 2143) [22]. The strength of Brønsted acidic sites (BASs) was estimated by the method of hydrogen bonds based on the change in the stretching vibration frequency of the OH groups that occurred under CO absorption. The higher the shift of OH stretching vibration, the stronger the acidity of this OHgroup. The shift of IR band of the acidic hydroxyls groups ($\Delta\nu_{OH}^{OH\cdots CO}$) were recalculated into the value of proton affinity (PA): PA[kJ/mol] = 1390−442.5* $\log_{10}(\Delta\nu_{OH}^{OH\cdots CO})/(\Delta\nu_{OH}^{SiOH\cdots CO})$ where 1390 kJ/mol corresponds to the PA of surface OH groups of Aerosil [22]. The concentration of BASs were determined from the intensity of the bands attributed to corresponding OH–group in the H-complex with the CO molecule (A_0 = 27 cm/μmol). In the presented spectra, the absorbance was normalized to sample wafer density (g/cm^2).

3.5. The methodology of UV–vis DRS

UV–vis diffuse reflectance spectra (UV–vis DRS) of the of the oxide CoMo catalysts and bulk reference samples were recorded using a UV-2501 PC Shimadzu spectrometer with an IRS-250A diffusion reflection attachment in the 11000–54000 cm^{-1} range. The measurements were performed in a 2 mm quartz cell in air at room temperature using the $BaSO_4$ as a reference. The edge energy (or band gap, Eg) for allowed transitions was determined by finding the intercept of the straight line for the low-energy rise of a plot of $[F(R_\infty) h\nu]^2$ versus $h\nu$ [24], where $h\nu$ is the incident photon energy, $F(R_\infty)$ is the Kubelka-Munk function.

3.6. Temperature-programmed desorption of the adsorbed CO_2

The basic properties of catalysts were characterized by using the temperature-programmed desorption of CO_2. The catalyst samples (0.25–0.35 g) were treated at its calcination temperature (550°C) in helium flow for 1 h and then saturated pure CO_2 flow after cooling to100°C. After removing weakly physisorbed CO_2 by purging with helium at 100°C for 1 h, the samples were heated to 550°C at a rate of 10°C/min in a helium flow (30 cm^3/min). The amount of base sites on the catalyst surface was calculated from the desorption amount of CO_2, which was determined by measuring the areas of

the desorption profiles from the «Micromeritics» AutoChem-2920 precision chemisorption system analyzer.

4. Results and discussion

4.1. Textural characteristics

Characteristic isotherms of nitrogen adsorption-desorption are given in Fig. 1. The samples of the supports and catalysts differ significantly in textural characteristics. According to widely known classifications [25–27], nitrogen adsorption-desorption isotherms of γ-Al$_2$O$_3$ and CoMo/γ-Al$_2$O$_3$ (Fig. 1) refer to IV type and contain hysteresis loop of H1 type. Consequently, the samples based on γ-Al$_2$O$_3$ have cylindrical type of pores. Nitrogen adsorption-desorption isotherms of ASA containing supports and catalysts refer to IV type (mesoporous materials) and contain hysteresis loop of H3 type independent to the way of Mg addition. H3 type of hysteresis loop is characteristic for slit-shaped pores. The form of hysteresis loops is similar for catalysts and their supports independent to catalyst composition. Therefore, sulfide active component particles localize uniformly in pores of the support and do not block pore mouth in all cases.

Plots of pore size distribution (Fig. 2) show a significant difference between the samples. The support and the catalyst based on γ-Al$_2$O$_3$ have a narrow pore size distribution with advantageous to pores in the range of 5–15 nm. Supporting of active metals (Co and Mo) decreases the volume of pores with the diameters of 5–11 nm, which indicates a localization of the active metal in these pores. In contrast to the samples with γ-Al$_2$O$_3$, all samples containing ASA have broad pore size distribution. According to nitrogen porosimetry (Table 1), the use of a support with ASA increases the surface area and pore volume. Consideration of the textural characteristics of the individual ASA and boehmite powders shows that the increase in the surface of the support in the CoMo/(Al + ASA), CoMoMg/AlASA and MgCoMo/AlASA is in proportion to ASA content in the carrier. Therefore, it can be assumed that no phase transitions, except boehmite $\rightarrow$ γ-Al$_2$O$_3$, does occur during preparation of the supports. Consequently, supports of the above-mentioned samples include ASA and γ-Al$_2$O$_3$ and contain no other phases.

Addition of Mg into ASA changes significantly textural characteristics. Surface of the support in CoMo/(Al + MgASA) is considerably lower in comparison with the sample without Mg. Also, there is the shift in the average pore diameter to lower values comparing to CoMo/(Al + ASA) catalyst. It can be proposed that changes of textural characteristics are caused by the formation of MgASA on the stage of deposition. This MgASA differs from the ASA without Mg. Obviously, MgASA particles have such properties that completely change interactions between particles of the support. These interactions form pores with low diameters and result in the low surface area. It should be noted that the support and catalyst in this case had low mechanical strength that indicate weak interactions between support particles. However, formed compounds are stable during hydrothermal treatment by Co-Mo impregnating solution that is confirmed by preservation of the form of pore size distribution plot of the catalyst as compared to a carrier. Therefore, it can be assumed that Mg, which is introduced into the ASA, forms a new compound with it and it is not present in the CoMo/(Al + MgASA) in the form of individual compounds, for example, oxide or hydroxide.

Addition of Mg at the stage of preparation of kneading paste also resulted in the decrease of surface area and pore diameter (Table 1). However, pore volume is slightly increases. Preservation of the form of pore size distribution plot also confirms the formation of stable Mg compounds in the support. These compounds do not change at the stages of impregnation and heat treatment. Possibly, Mg introduced to the support in the form of hydrotalcite like in [14]. Formation of hydrotalcite can be supposed because of the results obtained in [28], where the authors showed that impregnation of γ-Al$_2$O$_3$ by the solution of Mg compound leads to the growth of hydrotalcite on the surface of γ-Al$_2$O$_3$. In our case, there is the difference that Mg compound is added to the paste of the support and is subjected to peptization by nitric acid, extruding and thermal treatment. Mg was added as Mg(NO$_3$)$_2$ and possibly, there was exchange of OH$^-$ and NO^{3-} anions between Mg(NO$_3$)$_2$ and AlOOH. Therefore, in this case Mg should be in the form of MgO after calcination of the support. Thus, the difference in textural characterics between CoMo/(Al + ASA) and CoMo/(Al + Mg + ASA) should consist in the interation between MgO particles, ASA and γ-Al$_2$O$_3$.

Interesting in terms of textural characteristics are the samples with Mg, which was introduced by impregnating before or after Co and Mo. There is a significant drop in the specific surface area and the form of the plot of the pore size distribution. In the case of Mg addition before Co and Mo, it can be assumed that changes of textural characteristics are similar to that observed in [20,29], where it was shown that the main difficulty of using catalysts with Mg was instability of MgO during a contact with the impregnating solution. Thus, it was shown that the MgO was converted into Mg(OH)$_2$ in contact with the impregnating solution, which had a much smaller surface as compared with MgO. In addition, Mg(OH)$_2$ can form solid solutions with CoO and NiO, which impedes decoration of MoS$_2$ particles by atoms of the promoter. Thus, the transformation of Mg surface compounds can results in significant surface reconstructions during sequential deposition Mg $\rightarrow$ Co + Mo. In the case of Mg supporting after Co and Mo, surface restructuring due to redissolution and reprecipitation of Co and Mo compounds can also be assumed, as the Mg was supported by impregnating of the support by Mg(NO$_3$)$_2$ solution.

4.2. HRTEM

Surface characteristics of Co-Mo catalysts based on γ-Al$_2$O$_3$ are sufficiently studied and described in the literature. Prepared in this paper the catalyst for comparison (CoMo/γ-Al$_2$O$_3$) contains sulfide active component, which is uniformly distributed on the support surface (Fig. 3). Sulfide active component has the morphology similar to the Co-Mo-S phase in high active hydrotreating catalysts [30–32].

All samples of ASA catalysts are similar in surface structure and different considerably from CoMo/Al$_2$O$_3$. Three components can be identified in HRTEM images of sulfide catalysts: 1. ASA, 2. γ-Al$_2$O$_3$, 3. sulfide active component. Fig. 3 contains fragments of sulfide catalysts, which contain sulfide active component similar to CoMoS phase. Visible particles of active component were observed on γ-Al$_2$O$_3$ in all cases. ASA fragments contained only single visible particles of sulfide active component.

Morphology of active component depends significantly on the composition of the catalysts. Thus, CoMo/Al$_2$O$_3$ catalyst contains particles of sulfide active component with a stacking number of 1,6 and a length of 3,3 nm. Sulfide active component particles in catalysts with ASA have much higher stacking number (2.2 ÷ 2.9) and slab length (3.9–4.7 nm). Addition of Mg to ASA increases slightly stacking number, while average slab length of sulfide active component remains similar to the catalyst without Mg. Preservation of the morphology of active component in the case of Mg in ASA is expected enough, since the visible sulfide active ingredient is located on Al$_2$O$_3$. Thus, preservation of morphology indicates indirectly the absence of new phases in the support (other than γ-Al$_2$O$_3$ and ASA) and localization on γ-Al$_2$O$_3$, since the content of γ-Al$_2$O$_3$ and its own support surface remains unchanged.
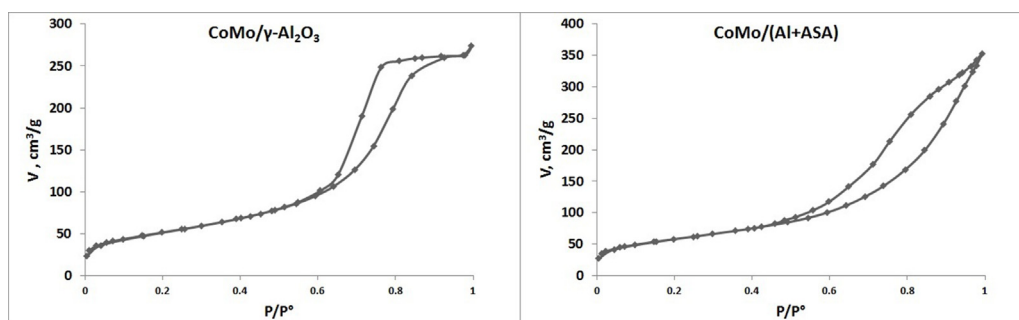
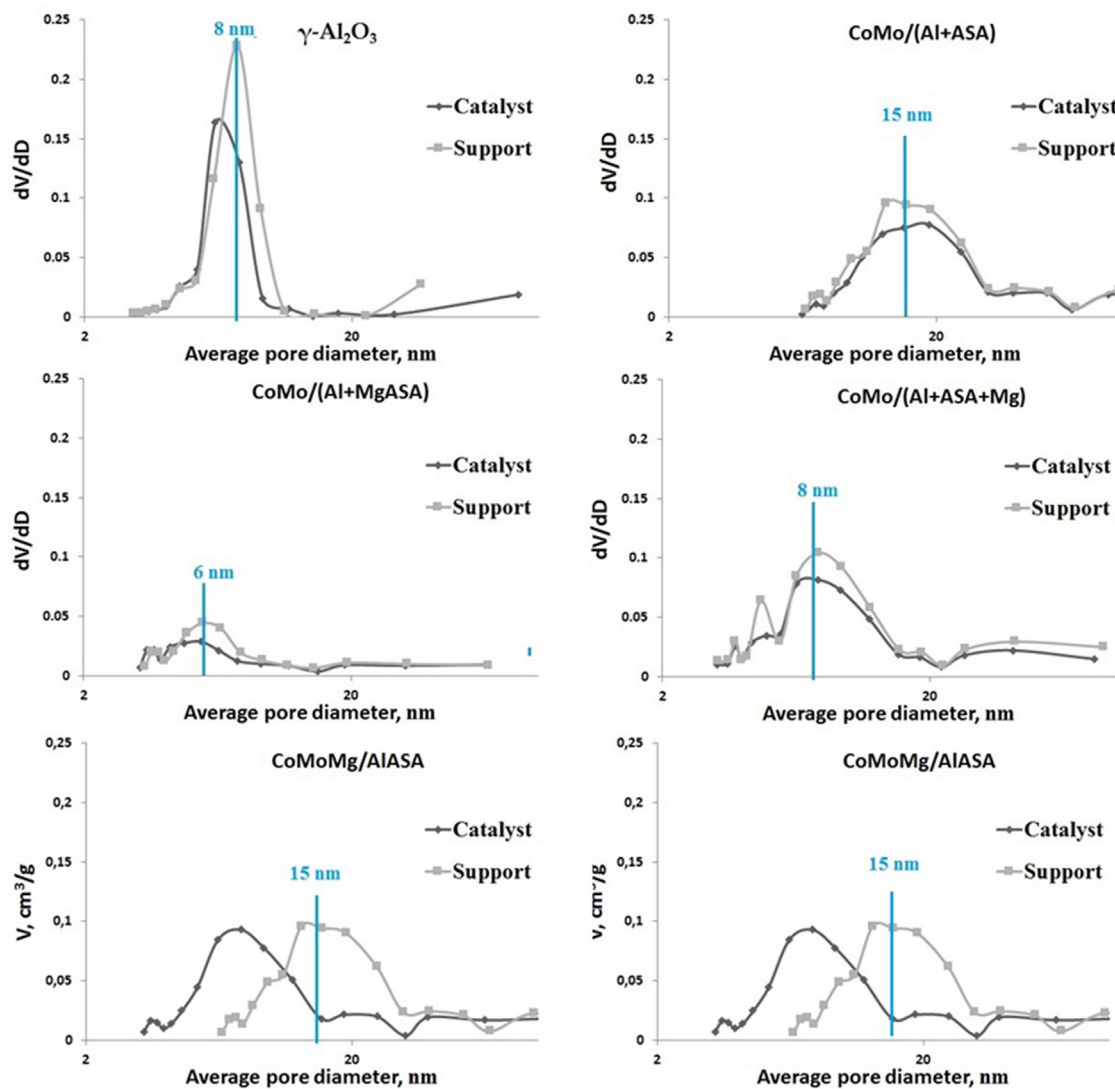Fig. 1. Isoterms of the nitrogen adsorption-desorption for CoMo/γ-Al$_2$O$_3$ and CoMo/(Al + ASA).

Fig. 2. Pore size distribution for supports and catalysts.

Table 1
Textural characteristics of supports and catalysts.

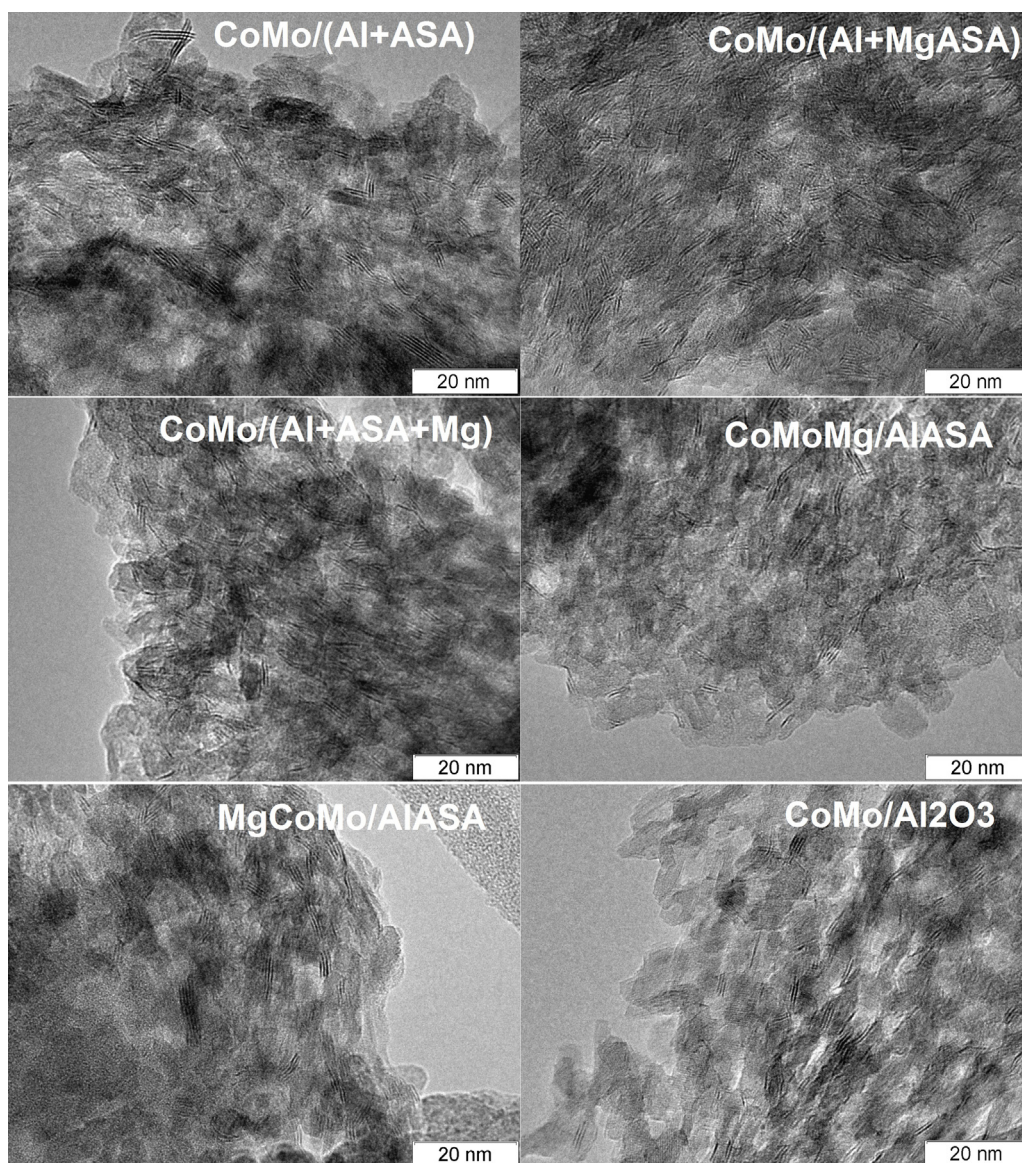| Sample	Support		Catalyst	
	Surface area, m^2/g	Pore volume, cm^3/g	Surface area, m^2/g	Pore volume, cm^3/g
CoMo/Al$_2$O$_3$	217	0.54	186	0.42
CoMo/(Al + ASA)	368	0.59	209	0.54
CoMo/(Al + MgASA)	293	0.41	216	0.33
CoMo/(Al + ASA + Mg)	312	0.63	259	0.52
CoMoMg/AlASA	368	0.59	234	0.54
MgCoMo/AlASA	368	0.59	214	0.55

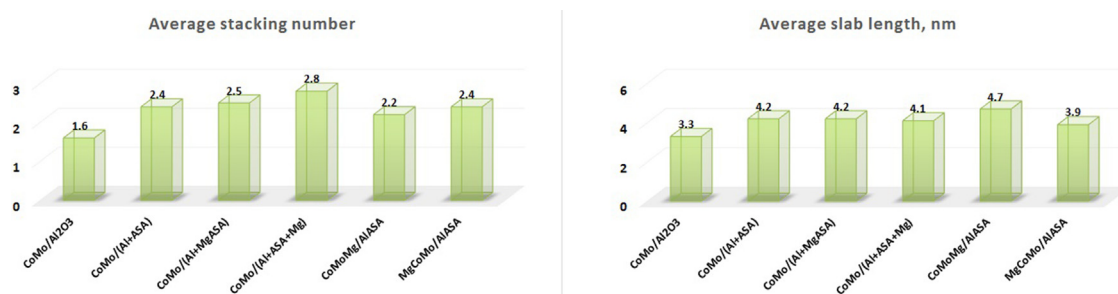**Fig. 3.** Fragments of HRTEM images of sulfide catalysts.

Fig. 4. Average stacking number and slab length of sulfide catalysts.

Introduction of Mg to the kneading paste results in a significant increase in the stacking number (Fig. 4). Therefore, Mg introduces to γ-Al_2O_3, since increasing of the visible sulfide active component particles does not observed. It can be assumed that the situation described in [20] is realized in this case, where the increase in the value of MoS_2 crystallites with increasing of Mg concentration was observed. Thus, it can be expected that CoMo/(Al + ASA + Mg) sam-

ple will have a higher selectivity in HDS/hydrogenation reactions due to the increased proportion of edge versus corner sites.

Addition of Mg before Co and Mo decreases slightly average slab length. However, morphology of the sulfide active component is very similar to CoMo/(Al + ASA). Addition of Mg in this case can be assumed to result in a negligible change of acid-base characteristics of γ-Al_2O_3 or Mg deposition on ASA. Given the observed changes in

the textural characteristics of the catalyst with a sequential impregnation Mg → Co and Mo, it can be assumed that the more likely Mg interacts preferentially with ASA and the possible transformations take place in this area.

The greatest impact of the introduction of Mg on the morphology of the sulfide active component is observed for CoMoMg/AlASA sample. There is a significant reduction of the amount of multilayer particles for this catalyst with increasing of average slab length (up to 4.7 nm). Consequently, there is a rearrangement of active component morphology at the second impregnation step of CoMo catalyst by the solution of $Mg(NO_3)_2$. Most probably, the interaction of the impregnating solution with CoMo catalyst results in the reconstitution of surface compounds followed by reprecipitation. It can be assumed that the degree of the promotion of MoS_2 particles, which are visible in HRTEM images, is lower in this case. However, visible particles of individual sulfide on the catalyst surface, as well as individual particles of Mg, do not observed.

4.3. XPS

XPS spectra of sulfide catalysts are rather uninformative as the content of the active metal sulfides (Co and Mo) is very low. Co2p spectra contain the peak in the range of 778.8 eV (Fig. 5 and Table 2). The peak is much widened due to the low amount of Co and, consequently, high noise level. However, binding energies values correspond to Co in sulfur-oxygene surrounding [33].

The band of S2p contains one peak at 162.0 ± 0.2 eV typical for S^{2-} form of sulfur in CoMoS catalysts [34,35]. However, the peak is significantly widened that could be due to the presence of S_2^{2-} form of sulfur in CoMoS catalysts [34,35]. The peak at 169,8 eV is caused by catalyst oxidation during the air storage. The sulfur peak has different intensity for the catalysts. The highest intensity is observed for CoMo/(Al + MgASA) catalyst. It is interesting that intensity of the peak is proportional to the intensity of the molybdenum peak in S2s + Mo3d spectra. Therefore, this sulfur is in Mo surrounding. Possibly, the sulfur in CoMo/(Al + MgASA) catalyst has the highest availability for the XPS method.

Significant changes can be seen in the spectra S2s + Mo3d. Despite the same Mg content in the catalysts (by chemical analysis), the intensity peaks of Mo varies (Fig. 6). Moreover, the intensity of the Mo lines correlates with the intensity of the lines in the spectra of S2p sulfide. All the spectra were deconvoluted. Deconvolution of Mo3d peaks was made to individual components (Mo^{4+}, Mo^{5+}, Mo^{6+}) similarly to [34,36]. The most representative spectra are given in Fig. 5. The data obtained are given in Table 2. The binding energy of $Mo3d_{5/2} = 228.7$ eV corresponds to Mo^{4+} state. It is characterized for molybdenum in sulfur surrounding in sulfide catalysts [37]. The most intensive lines of Mo3d were obtained for CoMo/(Al + ASA), CoMo/(Al + MgASA) and MgCoMo/AlASA that indicates minimal influence of Mg on Mo sulfide in the catalysts. Whereas the spectra of the samples, in which Mg was introduced into the support during kneading or after impregnation by Co and Mo compounds have the lowest intensity. If a correlation between the XPS and HRTEM data are made, it can be seen that the samples with the greatest impact of the Mg on the electronic state of S and Mo will show the greatest changes in the morphology of the active component. One would assume that the change in the intensity of the lines indicates not complete sulfiding of Mo. However, deconvolutions of the spectra showed that the content Mo^{4+} state, which is often corresponded to CoMoS phase) is in the range of 65–74%. Such values are typical for high active hydrotreating catalysts with complete sulfiding of active metals [37]. Moreover, Mo oxide particles were not detected visually in the HRTEM images. Decrease of the intensity may be due to a decrease of Mo availability to the electron beam due to the overlapping by other elements. However, Mg content is not so high to cause such effect., the Formation of

new Mg-Mo compounds or introduction of Mo into the carrier are most likely in this case.

The Al2p and Si2p spectra contain single peaks of equal intensity that indicate preservation of the electronic state of elements in the support independent to the way of Mg addition, since the Mg content is low. Si containing compounds are characterized by the lines in Si2p spectra in the binding energy range of 103.3–103.5 eV. The presence of the line in Si2p spectra of ASA catalysts with lower binding energy (102.5 eV) indicates the formation of silica oxide compounds with lower oxide state, e.g. SiOx or SixAlyOz. Therefore, Si in all studied samples presents in the form of mixed oxides or in the form of alumina-silica oxide compounds that confirms the formation of aluminosilicates.

Changes in Mg state are difficult to indicate because of the low Mg content and low intensity of spectral lines. However, broadening of the peaks for Mg containing samples suggests a superposition of two peaks of MgO with a binding energy of 50.1–50.3 eV and $MgCO_3$ with a binding energy of 51.3–51.6 eV. The presence of $MgCO_3$ can be explained by the conversion of MgO catalysts at long-term storage in the air [38]. It should be clarified that catalysts were transferred into the reactor without contact with air after sulfiding for catalytic activity tests, so the probability of a CO_2 sorption in catalysts with Mg as carbonate was lowered. On the other hand, it can be assumed that Mg forms compounds with Al_2O_3 or ASA that is confirmed by broadening of the peak at 50.0–50.4 eV [39]. However, it is difficult to assert the presence of Mg in any particular state.

4.4. IR-spectroscopy

It is known that the use of CO as a probe molecule to study sulfide catalysts is usually made to differentiates promoted and unpromoted sites well [40]. It was shown in [15] that modifying by Mg results in some important modifications on the sulfide phase. However, the amount of Mg and active metals (Co and Mo) is extremely low. Therefore, the difference in a promotion of active metals by will not be observed. In this study we concentrated on the influence of acid-base properties by Mg. Consequently, all catalysts have been studied by in the oxide form because Acid properties of the support does not significantly changed during the sulfiding

The IR spectra of ASA (Fig. 7) reveals several types of hydroxyl groups with the characteristic adsorption bands: the strong signal at 3747 cm^{-1} belongs to the terminal silanol groups (Si–OH); the shoulder at 3740 cm^{-1} corresponds to strongly acidic silanol OH groups typical for aluminosilicates that are located in the close vicinity of the Lewis acid site (e.g., tricoordinated Al atom) [41]; the shoulder at 3720 and 3670 cm^{-1} can be attributed to the Al—O(H)—Al groups and the broad-band at 3500–3600 cm^{-1} is attributed to hydroxyl groups, perturbed by hydrogen bond with vicinal OH groups. The absorbance band at 3670 cm^{-1} is observed as the very small peak, however, this band is well seen in the difference spectrum (Fig. 7). After deconvolution of the ASA spectrum into individual Gauss components, the concentration of different hydroxyl groups was evaluated from the integral intensity of corresponded bands ($A_0 = 3.5$ cm/μmol [42]) (Table 3). The IR spectrum of unmodified CoMo/ASA catalyst shows significant decrease in the peak intensity of unassociated Si-OH groups (almost doubly) that can result from dilution after supports formation and from the sorption of active component on these types of OH-groups. There is a greater decrease in the concentration of unassociated hydroxyl groups (Table 3) in the case of the samples with Mg. Modifying of support extrudates (MgCoMo/AlASA and CoMoMg/AlASA samples) is accompanied by the greater decrease in concentration of unassociated hydroxyl group than modifying of ASA (CoMo/(Al + MgASA)) or kneading paste by Mg (CoMo/(Al + ASA + Mg)).
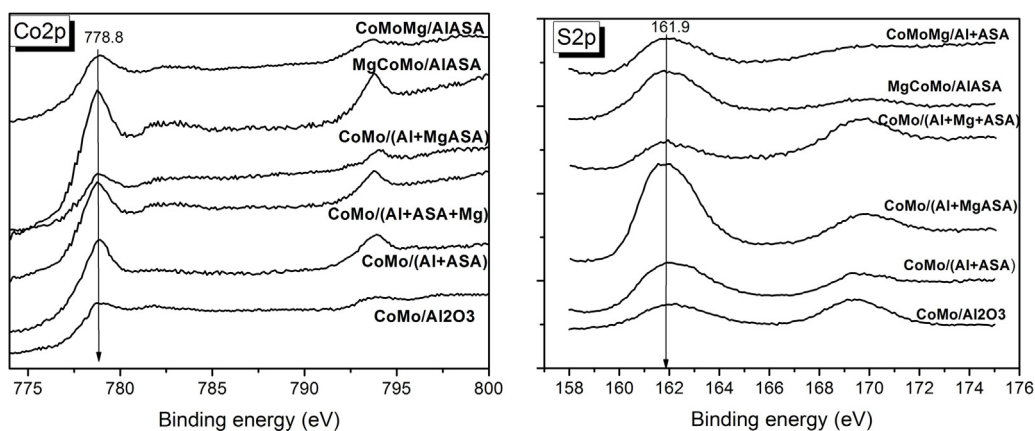
Fig. 5. Co2p and S2p XPS spectra of sulfide catalysts.

Table 2
XPS data for sulfide catalysts.

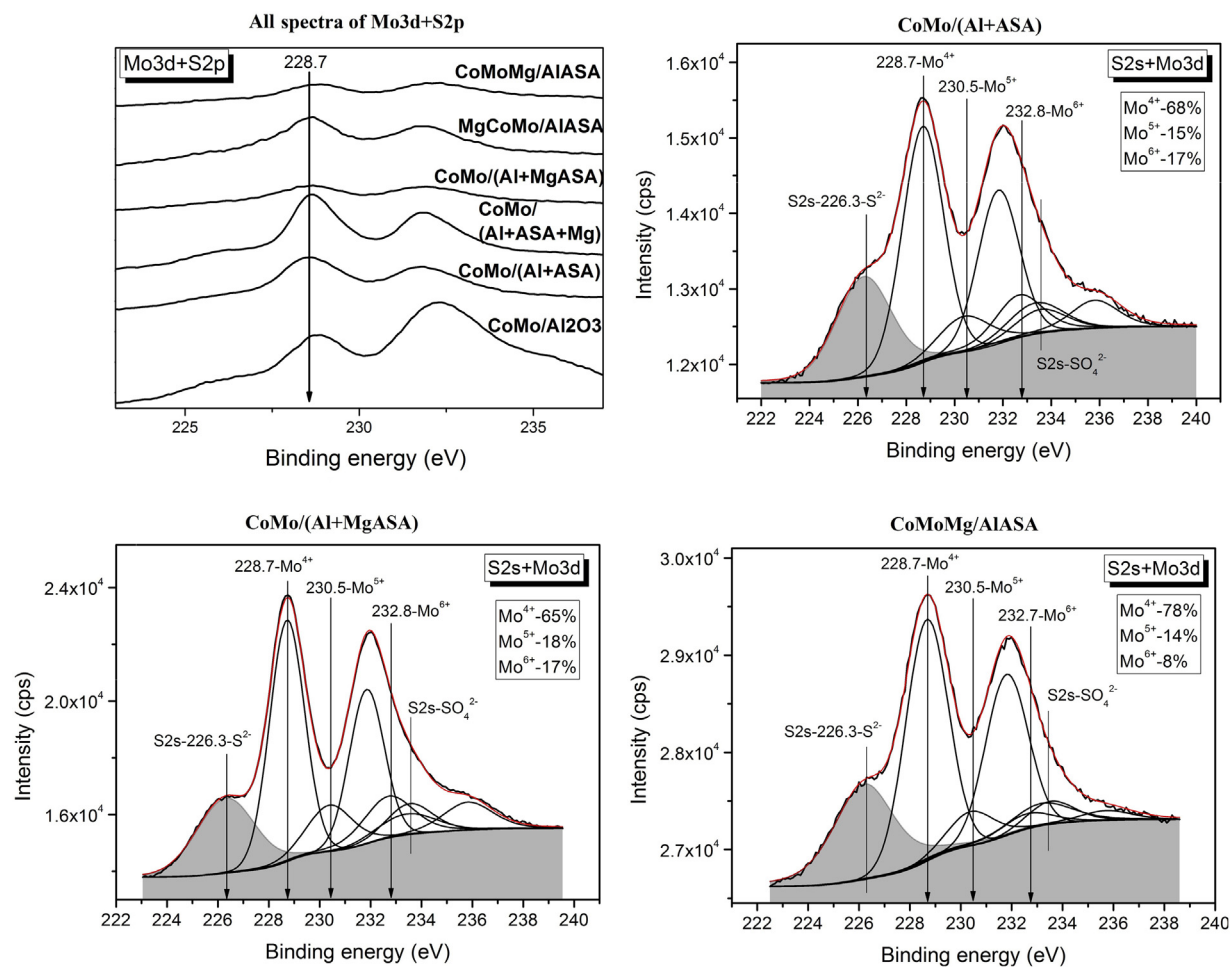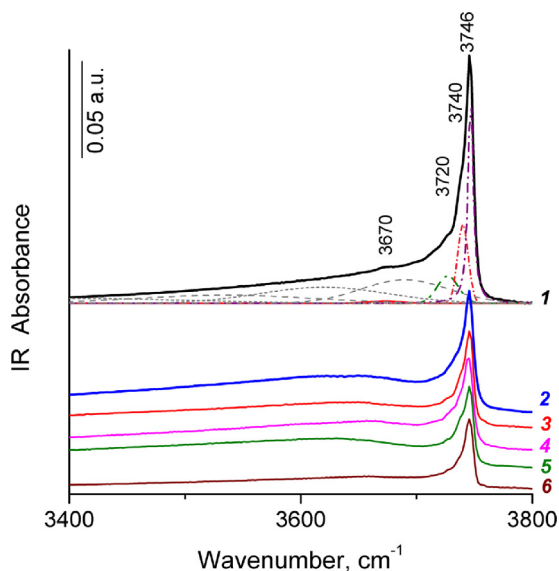|	CoMo/Al$_2$O$_3$	CoMo/(Al + ASA)	CoMo/(Al + MgASA)	CoMo/(Al + Mg + ASA)	MgCoMo/AlASA	CoMoMg/AlASA
BE, Mo 3d (eV)	229.1 ± 0.1	228.7	228.7	228.7	228.7	228.7
Mo^{4+} (%) MoS$_2$	55	68	65	70	78	74
Mo^{5+} (%)	16	15	18	14	14	18
Mo^{6+} (%)	29	17	17	16	8	8
BE, Co 2p (eV)	778.8 ± 0.1					
BE, S 2p (eV)	161.9 ± 0.2					
BE, Mg 2p (eV)	51.4 ± 0.2					

Fig. 6. Mo3d + S2p XPS spectra of sulfide catalysts.

Table 3
Concentration of some unassociated hydroxyl groups on ASA and catalysts surface.

| Type of sites	Si-OH terminal	Si-OH in the vicinity of the LAS	Al-O(H)-Al
ν_{O-H}, cm^{-1}	3746	3740	3720–3725
Sample	Concentration, μmol/g (Ao = 3.5 cm/μmol).		
ASA	250	135	92
Co-Mo/(Al + ASA)	130	57	57
Co-Mo/(Al + MgASA)	95	50	43
Co-Mo/(Al + ASA + Mg)	104	44	38
MgCoMo/AlASA	86	43	25
CoMoMg/AlASA	84	29	25

Fig. 7. IR spectra of ASA (1) and magnesium modified Co-Mo/ASA catalyst in the OH region: (2) CoMo/(Al + ASA), (3) CoMo/(Al + ASA + Mg), (4) CoMo/(Al + MgASA), (5) MgCoMo/AlASA, and (6) CoMoMg/AlASA. (Dash lines – decomposition of the spectrum of ASA sample).

Adsorption of carbon monoxide on ASA samples at liquid nitrogen temperature results in the shift of OH bands to the lower frequency region ($\Delta\nu_{OH}^{OH\cdots CO}$) due to perturbation of OH stretch by hydrogen bonding with CO molecule. The shift of OH groups with ν_{OH} 3670 cm^{-1} is 280 cm^{-1} (PA = 1170 kJ/mol); the shift of OH groups with ν_{OH} 3740 cm^{-1} is 260 cm^{-1} (PA = 1185 kJ/mol) (Fig. 8a). The first absorbance band can be attributed to acidic bridge Al—O(H)—Al group (BAS I), the second band can be attributed to acidic silanol OH groups that are located in the close vicinity of the LAS, such as Si—OH$\cdots$Al^{3+} (BAS II). In addition, the IR spectra after CO adsorption contain $\nu_{OH}^{OH\cdots CO}$ band at $\sim$3580–3600 and 3655 cm^{-1} due to disturbance of bridge Al—O(H)—Al (ν_{OH} = 3700–3720 cm^{-1}) and terminal Si—OH groups (ν_{OH} = 3747 cm^{-1}). There is a simultaneous appearance of the peaks at 2175–2178 and 2170 cm^{-1} in carbonyl region of the spectra (Fig. 8b), which can be attributed to CO complex with BASs.

The surface of CoMo/Al$_2$O$_3$-ASA catalysts contain the same types of BASs as initial ASA. Concentration of BASs is given in Table 4. BASs content in Co-Mo/(Al + ASA) is about 2/3 from the ones in initial ASA. It indicates that BASs are not involved in binding the active component. There is a decrease of BASs concentration for other samples. Obviously, it is associated with modification by Mg. Mg has the least impact upon introduction into ASA and highest after introduction by impregnation.

According to the IR data of adsorbed CO, the three types of the Lewis acid sites are observed on the surface of the ASA. The adsorption of CO (Fig. 8b) on the sample leads to the appearance of the following absorbance band: (1) peaks at 2230 and 2223 cm^{-1} corresponding to strong LAS relating to CO complexes with Al^{3+} ions in pentahedral environment being typical structural defects of ASA and zeolites, (2) signals at 2215 and 2207–2206 cm^{-1} corresponding to LAS of medium strength relating to CO complex with Al^{3+} ions, probably, in the aluminum oxide clusters, (3) bands at 2197 и 2185 cm^{-1} corresponding to weak LAS. Acid sites concentrations are summarized in Table 4.
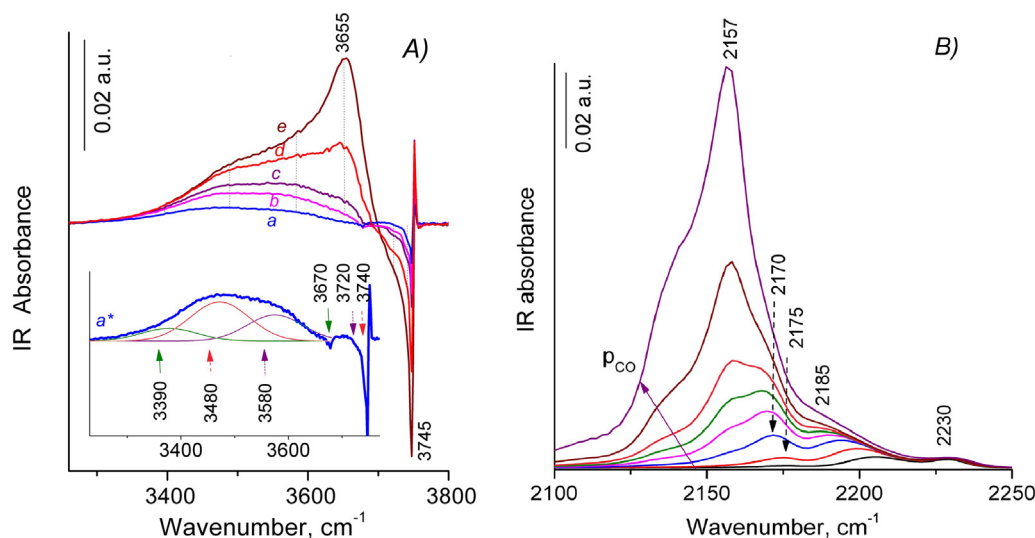
Fig. 8. IR difference spectra for ASA between the initial one and those with increased dosage of adsorbed CO at liquid nitrogen temperature: A) In the OH-region: (a, a*) P$_{CO}$ = 0.5 mbar; (b) P$_{CO}$ = 0.7 mbar; (c) P$_{CO}$ = 1 mbar; (d) P$_{CO}$ = 2 mbar and (e) pCO = 5 mbar. Inset shows the deconvolution of the spectrum (a). B) In the carbonyl region: CO pressures increased from 0.1 (bottom curve) to 13 mbar (top curve).
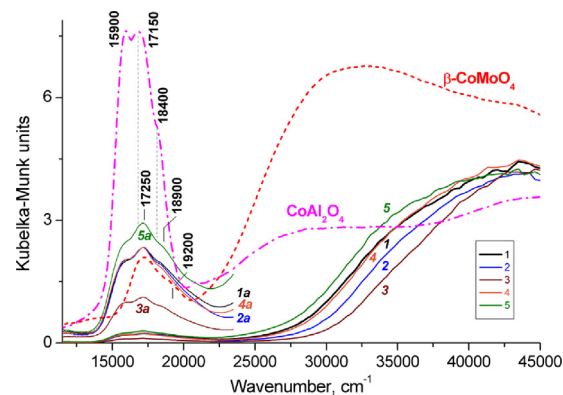
Table 4
Type, concentration (μmol/g) and strength of acid sites according to FTIR of adsorbed CO.

Type of sites	Brønsted acidic sites			Lewis acidic sites			
	Type I	Type II		Week**	Medium	Strong	
ν, см$^{-1}$	3670	3740	Σ BAS	2180–2198	2205–2215	2223–2230	Σ LAS, Al^{3+}
The strength of sites*, kJ/mol	PA = 1170	PA = 1185		Q_{CO} = 29–38	Q_{CO} = 41.5–46.5	Q_{CO} = 51.5–54	
Sample	Concentration, μmol/g						
Initial ASA	13	47	60	230	52	27	309
CoMo/(Al + ASA)	10	29	39	161	39	14	214
CoMo/(Al + MgASA)	9.5	26	35.5	220	43	23	286
CoMo/(Al + ASA + Mg)	5	20	25	177	31	12	220
MgCoMo/AlASA	4.5	15	19.5	130	21	8	159
CoMoMg/AlASA	4.5	17	21.5	197	33	18	248

* – Q_{CO} – heat of CO adsorption; PA – proton affinity.
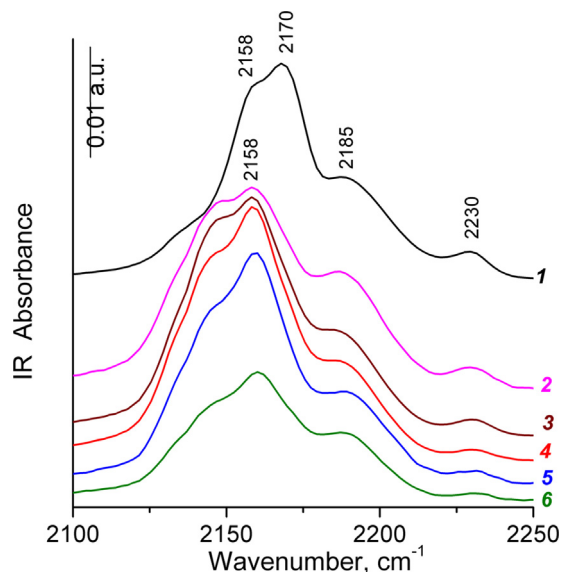
Fig. 9. IR spectra in the region of stretching vibrations of carbonyl groups of CO (5 mbar) adsorbed at liquid nitrogen temperature on ASA (1) and catalysts samples: CoMo/(Al + MgASA) (2); CoMoMg/AlASA (3); CoMo/(Al + ASA + Mg) (4); CoMo/(Al + ASA) (5); MgCoMo/AlASA (6). All spectra are background subtracted.

Fig. 10. UV–vis DR spectra of CoMo/(Al + ASA) (1), CoMo/(Al + MgASA) (2), CoMoMg/AlASA (3), CoMo/(Al + ASA + Mg) (4), MgCoMo/AlASA (5) catalysts and massive CoAl$_2$O$_4$ supplied by Aldrich and β-CoMoO$_4$ (the samples was synthesized in the laboratory). The spectra 1a–5a are multiplying by 10.

The comparative IR spectra of CO absorbed on the ASA and series of catalysts are given in Fig. 9. The types of Lewis acid sites of the catalysts according to CO adsorption at liquid nitrogen temperature are close to the sites of initial ASA. Additional bands at 2179–2180 cm^{-1} corresponding to weak LAS were defined in the spectra of the catalysts. Weak and medium LAS of catalysts are likely to be the sum of alumina and ASA sites. It was not possible to attribute some of the observed bands to CO complex with Mg^{2+} ions. The main feature of IR spectra of CO adsorption at room temperature on catalysts is the presence of the band at 2194–2192 cm^{-1}. This signal is supposed to attribute to the complex of CO with Co^{2+} ions [11]. This fact was taken into account below when LAS concentration was calculated.

It is found that the concentration of the LASs depends strongly on the way of Mg addition to the catalyst. Concentration of weak LASs in CoMo/(Al + MgASA), CoMo/(Al + ASA + Mg) and CoMoMg/AlASA catalysts exceeds concentration of LASs in CoMo/(Al + ASA). Perhaps, this excess is due to the presence of additional Lewis sites – ions of Mg^{2+}. Concentration of LASs in CoMo/(Al + ASA + Mg) catalyst is similar to the concentration of LASs in CoMo/(Al + ASA), although Mg content in this sample is maximal. It is possible that this is due to the fact that this method of Mg addition is not uniformly distributed and forms MgO. The lowest concentration of all types of LASs is observed for MgCoMo/AlASA catalyst. This may be caused by either a change in the surface of the sample or with the

healing of support defects during impregnating by a magnesium-containing solution followed by heat treatment.

The concentration of surface ions of Co^{2+}, which was defined from integral intensity of band at 2194-2192 cm^{-1} in room temperature IR spectra, was similar for CoMo/(Al + ASA), CoMo/(Al + MgASA) and CoMo/(Al + ASA + Mg) – 48 μmol/g (Ao = 0.5 cm/μmol [23]). This concentration is slightly lower for CoMoMg/AlASA catalyst – 39 μmol/g, which is possibly due to the fact that magnesium is introduced after active component. The concentration of surface ions of Co^{2+} for MgCoMo/AlASA catalyst is the lowest (28 μmol/g) that corresponds to the lowest concentration of all types of LASs for this sample.

4.5. UV–vis DO

The DRS spectra of dehydrated CoMo/ASA-Al$_2$O$_3$ catalysts in the oxides state are presented in Fig. 10. The intense adsorption band at about 45000–35000 cm^{-1}, recorded for CoMo samples, could be assigned to the ligand-metal charge transfer (CT) transitions O^{2-} → Mo^{6+}. The CT band centered at around 45000–44000 and 36000–35000 cm^{-1} for all Co-Mo/ASA-Al$_2$O$_3$ samples can indicate the presence of isolated tetrahedral coordinated Mo sites and polymolybdate-like structure containing Mo$_{Oh}$ ions, correspondingly [43]. The absorption edge of unmodified CoMo/(Al + ASA) catalyst is found to span a 3.95 eV range. The blue shifts of the absorption edge of molybdenum polyhedra in the spectra of CoMo/(Al + MgASA) (4.14 eV), CoMoMg/AlASA (4.36 eV), and CoMo/(Al + ASA + Mg) (4.00 eV) catalysts can be explained by changes in the average particle size (domain) of molybdenum oxide species in these catalysts in comparison with unmodified CoMo/(Al + ASA) catalyst. It is known that alkaline metals like sodium can decrease average domain size of the molyb-

denum containing nanoparticles [44]. However, HRTEM data show the increase of stacking number or average slab length of sulfide particles in our case. The greatest influence on average size of molybdenum containing nanoparticles is observed for CoMoMg/AlASA. The lowest influence of Mg is observed for CoMo/(Al + ASA + Mg). The red shifts of the absorption edge of molybdenum polyhedra in the spectra of MgCoMo catalyst (3.77 eV) can be attributed to smaller aggregates of molybdenum oxide domains in this catalyst [45].

In addition to the CT bands due to Mo appearing in the UV region, the visible spectra of these catalysts exhibit bands in the 20000–14000 cm^{-1} region, which are associated with Co species. In the spectra of all samples, a triplet of bands at about 15900, 17250 and 18900 cm^{-1} with the week shoulder at 19600 cm^{-1} was detected. The triplet at 15900, 17150 and 18400 cm^{-1} was found in $CoAl_2O_4$ [46,47] and attributed to d–d transitions Co^{2+} ions in a tetrahedral coordination. The bands at 17300 and 19200 cm^{-1} belongs to the characteristic peak of d–d transitions of high spin octahedral Co^{2+} complexes in β-$CoMoO_4$ [47,48]. It can be assumed that cobalt in catalysts is in both β-$CoMoO_4$ and $CoAl_2O_4$ structures.

The intensity of the peaks at 15900, 17250 and 18900 cm^{-1} in the spectra of catalysts depends on the way of Mg addition to the catalyst. Significant decrease of the peak intensity is observed for CoMoMg/AlASA. On the contrary, there is an increase of signal intensity for MgCoMo/AlASA. It is known that the bands of octahedral cobalt are much less intensive than those of tetrahedral cobalt and in situations where octahedral and tetrahedral cobalt occur together, the stronger bands of tetrahedral cobalt will cover the weaker bands of octahedral cobalt [47]. Although estimating the relative amounts of $CoAl_2O_4$-like Co^{2+} species and β-$CoMoO_4$ is quite difficult, the weakened triplet in the spectra of CoMoMg/AlASA catalyst may suggest an increased contribution of β-$CoMoO_4$ species. While the increase of triplet intensity in the spectra of MgCoMo/AlASA catalysts may characterized the increase of interation of active component and the support with a formation of inactive $CoAl_2O_4$-like cobalt species.

4.6. Catalytic activity

Sulfided catalysts were tested in hydrotreating of model fuel. Catalytic activity was estimated by two parameters: 1. desulfurization of thiophene, 2. research octane number, which was calculated according to the product composition. The results obtained are given in Table 5.

All catalysts have high desulfurization activity. When temperature of the reaction is 220°C, there is a slight difference in desulfurization activity. However, all catalysts achieved less than 10 ppm of sulfur in hydrotreated product at 240°C. Two catalysts CoMo(Al + Mg + ASA) and CoMoMg/AlASA and have the lowest sulfur content. It can be assumed that for these catalysts 10 ppm of sulfur content can be achieved at lower temperature than 240°C and this temperature will be lower than the one for other catalysts. It is known that decrease of temperature of the process for several degrees results in the increase of process efficiency. The highest sulfur content was obtained for CoMo/Al$_2$O$_3$ and MgCoMo/AlASA. CoMo/(Al + ASA) and CoMo/(Al + MgASA) have intermediate activity in desulfurization.

Analysis of hydrotreated product composition showed that the highest content of low-octane paraffins was obtained for CoMo/Al$_2$O$_3$. Moreover, the higher temperature of the process, the higher content of paraffins. Practically no isoparaffins were observed for CoMo/Al$_2$O$_3$ sample. Introduction of ASA into the support decreases formation of low-octane paraffins, while the formation of some isoparaffins occurs. Possibly, some paraffins can turn into isoparaffins over ASA-containing catalysts.

Initial amount of terminal olefin (hexene-1) was 20 wt.%. After the reaction total content of olefins in hydrotreated product obtained over CoMo/Al$_2$O$_3$ catalyst was 13 wt.% at 220°C and decreased with the temperature increase. Practically all olefins were linear isomers of the hexene-1: cis-hexene-1 and $trans$-hexene-1. Hydrotreated products obtained over catalysts with ASA contained similar total amount of olefins at 220°C. However, increase of the temperature resulted in different behavior of catalysts. The main trend was the formation of branched olefins. Branched olefins are known to have lower activity in hydrogenation reaction. Formation of branched olefins is favorable, because they have higher octane numbers than terminal linear olefins. Moreover, isoparaffins obtained from branched olefins have higher octane numbers than linear paraffins. Summing of linear olefins, branched olefins and paraffins for all ASA catalysts show that initial hexene-1 is subjected to three reactions: 1. hydrogenation to linear paraffin, 2. isomerization to branched olefin or to linear olefin with trans- and cis- configurations, 3. isomerization to branched olefin followed by hydrogenation to isoparaffin.

Considering the composition of hydrotreated products revealed that inspight of high amount of linear olefins obtained over CoMo/Al$_2$O$_3$, octane number of hydrotreated products obtained over ASA-containing catalysts should be higher. RON number was calculated according to the formula: $ON = \frac{\sum_i v_i ON_i}{\sum_i v_i}$, where v_i − wt. content of i component determined from chromatographic analysis of model fuel, ON_i −octane number of I component. The results are given in Table 5. The research octane number of the model fuel was 97.2 points. According to calculations, octane number loss for CoMo/Al$_2$O$_3$ catalyst at 220°C was 1 point. Increase of the process temperature results in the increase of octane number loss up to 3.3 points at 240°C. Therefore, achievement of 10 ppm of sulfur is accompanied with significant loss of RON by more than 2 points that is not acceptable for hydrotreating of FCC gasoline. Introduction of ASA into support resulted in the increase of RON up to 1.1 points comparing to the initial model fuel. When the hydrotreated product contains less than 10 ppm of sulfur, RON loss is equal to 0. Then, all other catalysts were compared in RON at 240°C, because of the sulfur content less than 10 ppm. Addition of Mg into supports and catalysts increases RON of the hydrotreated products. Moreover, all Mg containing catalysts show increase of RON comparing to the initial model fuel. Increasing of RON is in the following order: MgCoMo/AlASA, CoMo/(Al + MgASA), CoMoMg/(AlASA) and CoMo/(Al + Mg + ASA). Therefore, the highest RON was obtained for the catalysts with Mg introduced into kneading paste and with Mg added after Co and Mo compounds. Of course, behavior of catalysts in hydrotreating catalyst will be much more complicated due to complex composition of the gasoline. However, the main trends will be saved. It can be concluded that catalysts with ASA have much higher potential in preservation of octane number of hydrotreated model fuel, while addition of Mg have a positive influence on catalyst activity in desulfurization of sulfur components and in hydrogenation and isomerization of high-octane olefins. As a result, the data on the residual sulfur content and calculated RON of hydrotreated products suggests that CoMo/(Al + ASA + Mg) and CoMoMg/(Al + ASA) show the best catalytic performance.

4.7. TPD of CO$_2$

The possible modification of the catalysts basicity due to the introduction of magnesium was estimated by means of temperature-programmed desorption (TPD) of CO_2 (Fig. 11). It is known that the presence of alkaline ions such as potassium can results in a marked increase of the basic properties of the support of Co-Mo/Al$_2$O$_3$ catalysts [15]. Figure x shows the CO_2-TPD curves

Table 5
Composition of hydrotreated products, sulfur content and calculated RON.

Compounds in hydrotreated products	CoMo/Al$_2$O$_3$		CoMo/(Al + ASA)		CoMo/(Al + MgASA)		CoMo/(Al + Mg + ASA)		MgCoMo/(Al + ASA)		CoMoMg/(Al + ASA)	
	Content of components (wt.%) in hydrotreated products obtained at different temperatures											
	220 °C	240 °C	220 °C	240 °C	220 °C	240 °C	220 °C	240 °C	220 °C	240 °C	220 °C	240 °C
Paraffins	6.0	9.2	1.3	1.3	0.8	1.1	1.4	1.8	1.5	1.4	1.3	1.5
Isoparaffins	≪0.1	≪0.1	0.9	1.5	0.4	0.9	0.4	0.6	0.2	1.0	0.3	0.8
Total content of olefins	13.1	9.5	12.4	6.2	13.4	8.4	14.8	9.4	12.9	7.2	13.2	8.1
Linear olefins	13.0	9.5	10.6	3.5	12.2	6.4	13.8	7.1	11.5	4.7	12.2	5.5
Branched olefins	≪0.1	≪0.1	1.8	2.7	1.2	2.0	0.9	2.2	1.4	2.5	1.6	2.7
Initial RON = 97.2												
RON	96.2	93.9	98.3	97.2	98.7	97.5	98.8	97.7	98.3	97.3	98.7	97.6
ΔRON = initial RON–RON of hydrotreated product	1	3.3	−1.1	0	−1.5	−0.3	−1.6	−0.5	−1.1	−0.1	−1.5	−0.4
Sulfur content	70	≪10	59	≪10	62	≪10	40	≪10	68	≪10	45	≪10
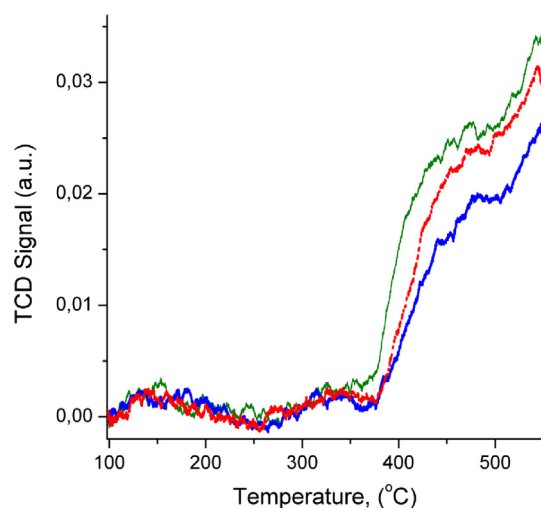
Fig. 11. CO$_2$-TPD profiles of (a) CoMoMg/AlASA, (b) CoMo/(Al + ASA) and (b) CoMo/(Al + ASA + Mg) samples.

of the CoMo/(Al + ASA + Mg), CoMoMg/AlASA and CoMo/(Al + ASA) samples in the oxide state. The first and second samples were studied due to the highest activity and selectivity in hydrotreating of model FCC gasoline. The strength of basic sites increases as the temperature of the peaks appeared in the TPD profile. The poor broad peak between 100 and 200 °C can be attributed to the interaction of CO$_2$ with the weak basic sites that correspond to residual basic hydroxyl groups on the surface. The second group between 200 and 370 °C most likely is associated with oxygen in the Mg^{2+} and O^{2-} pairs. Finally, those higher than 400°C could be due to the presence of strong basic sites, probably corresponding to isolated O^{2-} [49]. CO$_2$-TPD curves for the Mg modified catalysts CoMo/(Al + ASA + Mg), CoMoMg/AlASA and CoMo/(Al + ASA) sample without Mg show that the profile and the intensity of the signal slightly depend on the Mg presence. The amounts of CO$_2$ desorbed from CoMo/(Al + ASA + Mg), CoMoMg/AlASA and CoMo/(Al + ASA) samples are about 48, 56 and 54 μmol/g, respectively. It was suggested that modification by magnesium does not significantly increase the number of basic sites of the studied catalysts responsible for the CO$_2$ adsorption.

4.8. Influence of Mg on catalyst properties

The set of obtained results allows us to propose a model of the structure of the catalyst with the addition of Mg and without it (Fig. 12). The catalyst for comparison (CoMo/Al$_2$O$_3$) is a typical sys-

tem used in the hydrotreating of various petroleum distillates. The preparation method in the present article provides the catalyst with a uniform distribution of the active component on the support surface (preferably with one or two layers in the slab). Localization of the sulfide active component in ASA catalysts occurs preferentially on Al$_2$O$_3$. HRTEM images do not show localization of the sulfide active component on ASA. Moreover, reducing the content of Al$_2$O$_3$ in the composition of the support increases the stacking number and slab length. It indicates a reduction in uniformity of active component distribution in the catalyst. The free surface of ASA from the sulfide active component has a positive effect on the activity of catalysts in the isomerization of olefins and, as a consequence, on the selectivity of the catalysts.

The hydrotreating product obtained over CoMo/Al$_2$O$_3$ catalyst contained high amount of linear olefins and high amount of linear paraffins. Calculated octane number significantly decreased with the temperature increase that is undesirable. An addition of ASA to the support increased isomerization activity of the catalyst. The product obtained over CoMo/(Al + ASA) catalyst contained linear and branched olefins and linear and branched paraffins. It should be noted that branched olefins have lower activity in hydrogenating reactions and in most cases higher octane numbers than initial linear olefin. Brahched paraffins also have higher octane numbers that the linear ones. Therefore, the ASA presence provides maintainance of the octane number due to the formation of olefin derivatives with higher octane numbers. All ASA-containing catalysts provided less than 10 ppm of sulfur at 240 °C. In some cases it can be supposed that catalysts achieve 10 ppm of sulfur at lower temperatures due to low residual sulfur content at 220 °C. However, the catalysts have been compared at 240 °C taking into account calculated octane numbers.

Addition of Mg to ASA decreases surface area and pore volume of the catalyst that is most likely due to a change in the morphology of the ASA particles and the number of contacts between MgASA and Al$_2$O$_3$. The data on the acidity of the samples suggest the presence of Mg in the form of Mg^{2+} ions. There is no increase of HDS activity of the catalyst after the introduction of Mg^{2+} to the catalyst. However, calculated octane numbers of the hydrotreating products are higher that for CoMo/(Al + ASA). Probably high isomerisation function of the catalyst is associated with maximal amount of Lewis and Brønsted acid sites, while low HDS activity at 220°C is due to lower surface area and pore volume that decreases the active component dispersity.

Introduction of Mg before Co and Mo reduces significantly amount of acid sites. Probably, Mg is incorporated into a support in the form of Mg^{2+} ions. It slightly decreases the catalyst activity in HDS reaction. Octane numbers of the product are similar to the
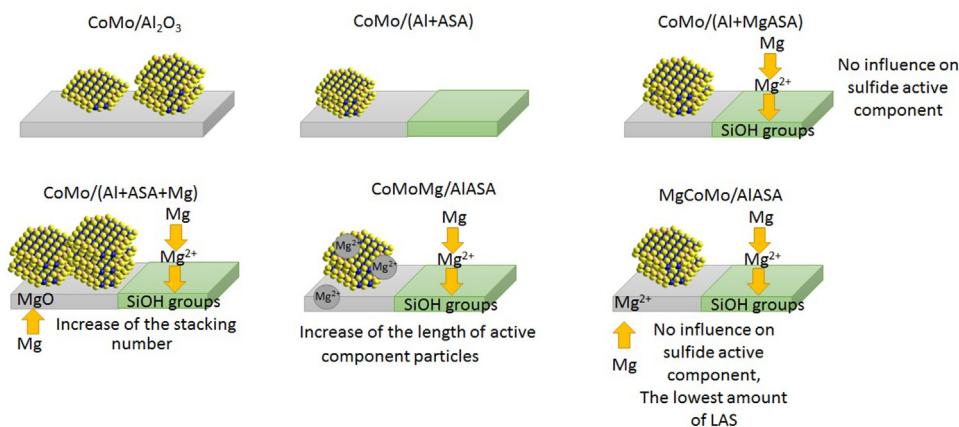
Fig. 12. Possible structure of catalysts with and without Mg.

ones of CoMo/(Al + ASA). Therefore, it is possible that Co and Mo covers Mg after supporting.

Introductions of Mg into the support at kneading stage and after Co and Mo have a very similar effect on the activity of the catalysts in HDS and HYD reactions. An interesting fact is that the catalysts are distinguished by the morphology of the sulfide active component, but are similar in the amount of LAS and BAS. The activity of catalysts in HDS is higher than that of CoMo/(Al + ASA) catalyst. It indicates high influence of Mg on sulfide active component. It may be assumed that Mg in the support CoMo/(Al + ASA + Mg) forms sites of definite acidity, which have an influence on localization of sulfide active component on the support surface, namely an increase in stacking number. Addition of Mg after Co and Mo, on the contrary, decreases stacking number and increases average length. In this case, mechanism proposed in [50] for the K-containing catalysts can be assumed. This mechanism suggests that Mg is introduced into the active phase and forms MgCoMoS phase. This phase has low HYD and high HDS activity. Interestingly, both catalysts have a very similar set of LAS and BAS acid sites. The main difference from the CoMo/(Al + ASA) catalyst is the reduced amount of week LAS that is probably due to a distribution of Mg in ASA. Therefore, we can assume that some increase in the amount of hydrogenation product, a reduced degree of isomerization and increased activity in HDS is associated with poisoning of LAS of ASA. Consequently, there is a possibility that if the Mg is added directly to boehmite prior to kneading step, the activity in HDS reaction will increase.

It is obvious that the introduction of Mg to ASA catalysts have a positive effect on the catalytic activity in HDS reactions. However, the method of Mg addition has a significant effect on the activity of the catalysts in the hydrogenation of olefins. CoMo/(Al + ASA + Mg) and CoMoMg/AlASA showed the best results from the viewpoint of the ratio of activities in the hydrodesulfurization and hydrogenation reactions. From our point of view, CoMo/(Al + ASA + Mg) is the best sample due to a smaller amount of technological steps used in the preparation.

5. Conclusion

The influence of Mg addition on properties of CoMo/Al$_2$O$_3$-ASA catalysts was studied in present work. Mg was introduced at different stages of catalyst preparation. It was defined that sulfide active component localized preferentially on Al$_2$O$_3$ independent to the way of Mg addition. It was shown that the way of Mg addition had a significant effect on the morphology of the sulfide active component, the textural characteristics and acid properties of the catalysts. Addition of Mg to the catalysts increases the activity in

the hydrodesulfurization of thiophene in all cases. However, the method of Mg introduction has a significant impact on the activity of the catalysts in hydrogenation and isomerization. The best results were obtained for the catalysts with addition of Mg into kneading paste and after Co and Mo as these catalysts showed the highest activity in the hydrodesulfurization and a lower – in hydrogenation. It was defined that the catalysts had a similar set of LAS and BAS and different morphology of the sulfide active component. The introduction of Mg into kneading paste of the support resulted in the highest stacking number, whereas introduction of Mg after Co and Mo resulted in the highest slab length. As a result, it was concluded that Mg had a positive effect on the activity and selectivity of catalysts based on amorphous aluminosilicates. The best method of Mg addition in terms of preparation is addition to the carrier at the kneading stage.

References

[1] S. Brunet, D. Mey, G. Pérot, C. Bouchy, F. Diehl, On the hydrodesulfurization of FCC gasoline: a review, Appl. Catal. A 278 (2005) 143–172.
[2] H. Topsøe, The role of Co–Mo–S type structures in hydrotreating catalysts, Appl. Catal. A 322 (2007) 3–8.
[3] T.G. Kaufmann, A. Kaldor, G.F. Stuntz, M.C. Kerby, L.L. Ansell, Catalysis science and technology for cleaner transportation fuels, Catal. Today 62 (2000) 77–90.
[4] J.T. Miller, W.J. Reagan, J.A. Kaduk, C.L. Marshall, A.J. Kropf, Selective hydrodesulfurization of FCC naphtha with supported MoS2 catalysts: the role of cobalt, J. Catal. 193 (2000) 123–131.
[5] Y. Fan, G. Shi, H. Liu, X. Bao, Morphology tuning of supported MoS2 slabs for selectivity enhancement of fluid catalytic cracking gasoline hydrodesulfurization catalysts, Appl. Catal. B 91 (2009) 73–82.
[6] M. Badawi, L. Vivier, G. Pérot, D. Duprez, Promoting effect of cobalt and nickel on the activity of hydrotreating catalysts in hydrogenation and isomerization of olefins, J. Mol. Catal. A: Chem. 293 (2008) 53–58.
[7] H. Qiherima, H.F. Yuan, Y.H. Li, G.T. Xu Zhang, Investigation on the active phase of CoMo catalyst for selective HDS by low temperature in situ FT-IR, Chin. Chem. Lett. 22 (2011) 366–369.
[8] A. Daudin, A.F. Lamic, G. Pérot, S. Brunet, P. Raybaud, C. Bouchy, Microkinetic interpretation of HDS/HYDO selectivity of the transformation of a model FCC gasoline over transition metal sulfides, Catal. Today 130 (2008) 221–230.
[9] Y. Okamoto, A. Kato, Usman, N. Rinaldi, T. Fujikawa, H. Koshika, I. Hiromitsu, T. Kubota, Effect of sulfidation temperature on the intrinsic activity of Co–MoS2 and Co–WS2 hydrodesulfurization catalysts, J. Catal. 265 (2009) 216–228.

[10] E.J.M. Hensen, P.J. Kooyman, Y. van der Meer, A.M. van der Kraan, V.H.J. de Beer, J.A.R. van Veen, R.A. van Santen, The relation between morphology and hydrotreating activity for supported MoS2 particles, J. Catal. 199 (2001) 224–235.

[11] K.A. Nadeina, O.V. Klimov, V.Y. Pereima, G.I. Koryakina, I.G. Danilova, I.P. Prosvirin, E.Y. Gerasimov, A.M. Yegizariyan, A.S. Noskov, Catalysts based on amorphous aluminosilicates for selective hydrotreating of FCC gasoline to produce Euro-5 gasoline with minimum octane number loss, Catal. Today 271 (2016) 4–15.

[12] D.J. Pérez-Martínez, E.M. Gaigneaux, S.A. Giraldo, A. Centeno, Interpretation of the catalytic functionalities of CoMo/ASA FCC-naphtha-HDT catalysts based on its acid properties, J. Mol. Catal. A: Chem. 335 (2011) 112–120.

[13] G. Muralidhar, F.E. Massoth, J. Shabtai, Catalytic functionalities of supported sulfides: i. Effect of support and additives on the CoMo catalyst, J. Catal. 85 (1984) 44–52.

[14] R. Zhao, C. Yin, H. Zhao, C. Liu, Synthesis, characterization, and application of hydotalcites in hydrodesulfurization of FCC gasoline, Fuel Process. Technol. 81 (2003) 201–209.

[15] D. Mey, S. Brunet, C. Canaff, F. Maugé, C. Bouchy, F. Diehl, HDS of a model FCC gasoline over a sulfided CoMo/Al2O3 catalyst: effect of the addition of potassium, J. Catal. 227 (2004) 436–447.

[16] Y. Fan, J. Lu, G. Shi, H. Liu, X. Bao, Effect of synergism between potassium and phosphorus on selective hydrodesulfurization performance of Co–Mo/Al2O3 FCC gasoline hydro-upgrading catalyst, Catal. Today 125 (2007) 220–228.

[17] D.J. Pérez-Martínez, P. Eloy, E.M. Gaigneaux, S.A. Giraldo, A. Centeno, Study of the selectivity in FCC naphtha hydrotreating by modifying the acid–base balance of CoMo/(-Al2O3 catalysts, Appl. Catal. A 390 (2010) 59–70.

[18] A.P. Yu, E.C. Myers, Selective hydrodesulfurization of cracked naphtha, Google Patents, 1979.

[19] P.S.E. Dai, D.E. Sherwood, R.H. Petty, Hydrodesulfurization of cracked naphtha with hydrotalcite-containing catalyst, Google Patents, 1994.

[20] T. Klimova, D. Solís Casados, J. Ramírez, New selective Mo and NiMo HDS catalysts supported on Al2O3–MgO(x) mixed oxides, Catal. Today 43 (1998) 135–146.

[21] S. Chen, T. Li, G. Cao, M. Guan, Amorphous silica-alumina, a carrier combination and a hydrocracking catalyst containing the same, and processes for the preparation thereof, Google Patents, 2002.

[22] E.A. Paukshtis, E.N. Yurchenko, Study of the acid–base properties of heterogeneous catalysts by infrared spectroscopy, Russ. Chem. Rev. 52 (1983) 242–258.

[23] R.I. Soltanov, E.A. Paukshtis, E.N. Yurchenko, IR spectroscopic investigation of the thermodynamics of the reaction of carbon-monoxide with the surface of several oxide adsorbents, Kinet. Catal. 23 (1982) 135–141.

[24] J. Tauc, R. Grigorovici, A. Vancu, Optical properties and electronic structure of amorphous germanium, Phys. Status Solidi (b) 15 (1966) 627–637.

[25] S. Brunauer, L.S. Deming, W.E. Deming, E. Teller, On a Theory of the van der Waals Adsorption of Gases, J. Am. Chem. Soc. 62 (1940) 1723–1732.

[26] K. Kaneko, Determination of pore size and pore size distribution: 1. Adsorbents and catalysts, J. Memb. Sci. 96 (1994) 59–89.

[27] D. Laurenti, B. Phung-Ngoc, C. Roukoss, E. Devers, K. Marchand, L. Massin, L. Lemaitre, C. Legens, A.-A. Quoineaud, M. Vrinat, Intrinsic potential of alumina-supported CoMo catalysts in HDS: comparison between γc, γT, and δ-alumina, J. Catal. 297 (2013) 165–175.

[28] J.J. Creasey, A. Chieregato, J.C. Manayil, C.M.A. Parlett, K. Wilson, A.F. Lee, Alkali- and nitrate-free synthesis of highly active Mg-Al hydrotalcite-coated alumina for FAME production, Catal. Sci. Technol. 4 (2014) 861–870.

[29] T. Klicpera, M. Zdražil, Preparation of high-activity MgO-supported Co–Mo and Ni–Mo sulfide hydrodesulfurization catalysts, J. Catal. 206 (2002) 314–320.

[30] Y. Okamoto, A. Kato, Usman, K. Sato, I. Hiromitsu, T. Kubota, Intrinsic catalytic activity of SiO2-supported Co–Mo and Co–W sulfide catalysts for the hydrodesulfurization of thiophene, J. Catal. 233 (2005) 16–25.

[31] Y. Okamoto, K. Hioka, K. Arakawa, T. Fujikawa, T. Ebihara, T. Kubota, Effect of sulfidation atmosphere on the hydrodesulfurization activity of SiO2-supported Co–Mo sulfide catalysts: local structure and intrinsic activity of the active sites, J. Catal. 268 (2009) 49–59.

[32] S. Eijsbouts, A.A. Battiston, G.C. van Leerdam, Life cycle of hydroprocessing catalysts and total catalyst management, Catal. Today 130 (2008) 361–373.

[33] S.K. Swami, N. Chaturvedi, A. Kumar, R. Kapoor, V. Dutta, J. Frey, T. Moehl, M. Grätzel, S. Mathew, M.K. Nazeeruddin, Investigation of electrodeposited cobalt sulphide counter electrodes and their application in next-generation dye sensitized solar cells featuring organic dyes and cobalt-based redox electrolytes, J. Power Sources 275 (2015) 80–89.

[34] A.D. Gandubert, E. Krebs, C. Legens, D. Costa, D. Guillaume, P. Raybaud, Optimal promoter edge decoration of CoMoS catalysts: a combined theoretical and experimental study, Catal. Today 130 (2008) 149–159.

[35] N. Frizi, P. Blanchard, E. Payen, P. Baranek, C. Lancelot, M. Rebeilleau, C. Dupuy, J.P. Dath, Genesis of new gas oil HDS catalysts: study of their liquid phase sulfidation, Catal. Today 130 (2008) 32–40.

[36] O.V. Klimov, K.A. Leonova, G.I. Koryakina, E.Y. Gerasimov, I.P. Prosvirin, S.V. Cherepanova, S.V. Budukva, V.Y. Pereyma, P.P. Dik, O.A. Parakhin, A.S. Noskov, Supported on alumina Co-Mo hydrotreating catalysts: dependence of catalytic and strength characteristics on the initial AlOOH particle morphology, Catal. Today 220–222 (2014) 66–77.

[37] M.A. Baker, R. Gilmore, C. Lenardi, W. Gissler, XPS investigation of preferential sputtering of S from MoS2 and determination of MoSx stoichiometry from Mo and S peak positions, Appl. Surf. Sci. 150 (1999) 255–262.

[38] V. Fournier, P. Marcus, I. Olefjord, Oxidation of magnesium, Surf. Interface Anal. 34 (2002) 494–497.

[39] G. Mattogno, G. Righini, G. Montesperelli, E. Traversa, XPS analysis of the interface of ceramic thin films for humidity sensors, Appl. Surf. Sci. 70 (1993) 363–366.

[40] F. Maugé, J.C. Lavalley, FT-IR study of co adsorption on sulfided Mo/Al2O3 unpromoted or promoted by metal carbonyls: titration of sites, J. Catal. 137 (1992) 69–76.

[41] A.A. Gabrienko, I.G. Danilova, S.S. Arzumanov, A.V. Toktarev, D. Freude, A.G. Stepanov, Strong acidity of silanol groups of zeolite beta: evidence from the studies by IR spectroscopy of adsorbed CO and 1H MAS NMR, Microporous Mesoporous Mater. 131 (2010) 210–216.

[42] E. Baumgarten, R. Wagner, C. Lentes-Wagner, Extinction coefficients of hydroxyl- and deuteroxyl groups on silica and alumina, Fresenius' Zeitschrift für analytische Chemie 335 (1989) 375–381.

[43] H. Jeziorowski, H. Knoezinger, Raman and ultraviolet spectroscopic characterization of molybdena on alumina catalysts, J. Phys. Chem. 83 (1979) 1166–1173.

[44] J.E. Herrera, D.E. Resasco, Loss of single-walled carbon nanotubes selectivity by disruption of the Co?Mo interaction in the catalyst, J. Catal. 221 (2004) 354–364.

[45] M. Fournier, C. Louis, M. Che, P. Chaquin, D. Masure, Polyoxometallates as models for oxide catalysts: part I. An UV-visible reflectance study of polyoxomolybdates: influence of polyhedra arrangement on the electronic transitions and comparison with supported molybdenum catalysts, J. Catal. 119 (1989) 400–414.

[46] M.L. Jacono, A. Cimino, G.C.A. Schuit, Gazzetta Chim. Ital. 103 (1973) 1281.

[47] J.H. Ashley, P.C.H. Mitchell, Cobalt-molybdenum-alumina hydrodesulphurisation catalysts. Part I. A spectroscopic and magnetic study of the fresh catalyst and model compounds, J. Chem. Soc. A (1968) 2821–2827.

[48] P. Gajardo, P. Grange, B. Delmon, Physicochemical characterization of the interaction between cobalt molybdenum oxide and silicon dioxide. 1. Influence of the cobalt-molybdenum ratio, J. Phys. Chem. 83 (1979) 1771–1779.

[49] Z. Liu, J.A. Cortés-Concepción, M. Mustian, M.D. Amiridis, Effect of basic properties of MgO on the heterogeneous synthesis of flavanone, Appl. Catal. A: Gen. 302 (2006) 232–236.

[50] D. Ishutenko, P. Nikulshin, A. Pimerzin, Relation between composition and morphology of K(Co)MoS active phase species and their performances in hydrotreating of model FCC gasoline, Catal. Today 271 (2016) 16–27.